



TITLE:

# Intrinsic crystalline structure of epitaxial Pb(Zr,Ti)O-3 thin films

AUTHOR(S):

Kanno, I; Kotera, H; Matsunaga, T; Wasa, K

---

CITATION:

Kanno, I ...[et al]. Intrinsic crystalline structure of epitaxial Pb(Zr,Ti)O-3 thin films. JOURNAL OF APPLIED PHYSICS 2005, 97(7): 074101.

ISSUE DATE:

2005-04-01

URL:

<http://hdl.handle.net/2433/50136>

RIGHT:

Copyright 2005 American Institute of Physics. This article may be downloaded for personal use only. Any other use requires prior permission of the author and the American Institute of Physics.

# Intrinsic crystalline structure of epitaxial $\text{Pb}(\text{Zr},\text{Ti})\text{O}_3$ thin films

Isaku Kanno<sup>a)</sup> and Hidetoshi Kotera

*Department of Mechanical Engineering, Kyoto University, Kyoto 606-8501, Japan*

Toshiyuki Matsunaga

*Matsushita Technoresearch Inc., Osaka 570-8501, Japan*

Kiyotaka Wasa

*Faculty of Science, Yokohama City University, Yokohama 236-0027, Japan*

(Received 13 July 2004; accepted 16 January 2005; published online 18 March 2005)

We report on the intrinsic crystalline structure of epitaxial ferroelectric  $\text{Pb}(\text{Zr},\text{Ti})\text{O}_3$  (PZT) films, which are fully relaxed from the stress of the substrate. The PZT films with the rhombohedral composition of  $\text{Zr}/\text{Ti}=68/32$  were epitaxially grown on (001)Pt/(001)MgO substrates. Four-circle x-ray diffraction measurements revealed that the films showed not only perfect *c*-axis orientation, but also a tetragonal phase due to a clamping effect of the substrate. Successively, x-ray diffraction measurements using synchrotron radiation were carried out to examine the intrinsic structure of stress-free PZT films, which were powdered after substrate removal. The structure refinement by Rietveld analysis demonstrated that the films without substrates returned to a rhombohedral phase, however, 19% of the B site in the perovskite structure was occupied by Pb atoms. The phase-transition temperature from rhombohedral to cubic slightly decreased due to the anomalous structure of the stress-free PZT films. These results suggest that the deviation of the thin-film properties from the bulk ones is caused not only by in-plane epitaxial stress as an extrinsic factor, but also by the anomalous crystalline structure of the stress-free thin films. © 2005 American Institute of Physics. [DOI: 10.1063/1.1871332]

## I. INTRODUCTION

Thin-film materials are essential for a variety of applications especially in microelectric devices, and lots of efforts have been employed to fabricate high-quality thin films emulating the properties of bulk materials. In recent years, not only metals or semiconductors but also functional ceramics have been fabricated as a thin-film form for integration into microdevices. However, thin films usually suffer significant compression or tensile stress due to a clamping effect of the substrates. The stress accumulated in thin films is considered as a major cause of the deformation of the crystalline structure from the original bulk ones and, furthermore, it leads to suppression (or enhancement) of the electric properties of the functional thin films.

In particular, high-temperature superconductors and ferroelectric oxides with a perovskite structure have attracted considerable attention due to their unique characteristics suitable for a variety of new functional microdevices. These perovskite materials can be grown as epitaxial films on single-crystal substrates such as  $\text{SrTiO}_3$  or  $\text{MgO}$ ; hence, we can not only eliminate the effects of grain boundaries but also optimize the crystalline orientation to enhance the specific properties of thin films. In both superconductive and ferroelectric thin films, epitaxial growth can be achieved on heated substrates, however, it induces a large internal stress in the resulting films because of the difference in thermal-expansion coefficients and the lattice mismatch. In the case of superconductors, it has been reported that the internal compressive

stress due to the epitaxial growth causes the increase of the critical temperature as well as the deformation of the band structure.<sup>1,2</sup> In general, lattice parameters of epitaxial films strongly depend on various conditions such as deposition process, film thickness, and substrates used.

Strain effect for ferroelectric thin films has been investigated intensively.<sup>3–5</sup> Wang *et al.* reported the enhancement of polarization and piezoelectricity for  $\text{BiFeO}_3$  epitaxial thin films, which show remarkable thickness dependence due to the epitaxial strain.<sup>6</sup> The relationship between the stress and the electric properties of the ferroelectric bulk materials has been studied using Landau–Devonshire’s phenomenological theory.<sup>7,8</sup> In the case of the thin films, discrepancy of the electric properties from the bulk ones was also studied using this theory.<sup>4,9</sup> However, we can adopt this theory for thin films only when the thin films should have the same crystalline structure as the bulk materials in the absence of the substrates. Since it is difficult to examine the crystalline structure of the stress-free ferroelectric films, the intrinsic crystalline structure of the thin films has not been investigated so far. In previous work, we etched out the substrates and then successively identified the crystalline structure of the stress-free  $\text{Pb}(\text{Zr},\text{Ti})\text{O}_3$  (PZT) thin films with a  $\text{Zr}/\text{Ti}$  composition of 57/43 by synchrotron x-ray diffraction (XRD) measurement.<sup>10</sup> In this measurement, we revealed their crystalline structure was still tetragonal even in the stress-free state.

In this study, we prepared epitaxial PZT thin films with further Zr-rich composition of  $\text{Zr}/\text{Ti}=68/32$  on the (001)Pt-coated (001)MgO single crystals and successively, the crystalline structure was measured in detail before and after sub-

<sup>a)</sup>Electronic mail: kanno@mech.kyoto-u.ac.jp

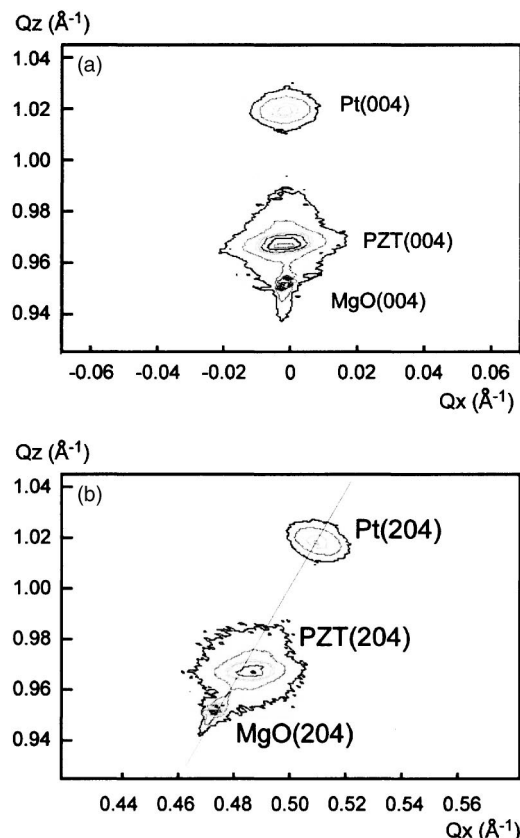


FIG. 1. Cu  $K\alpha$  x-ray diffraction patterns of the PZT (Zr/Ti=68/32) film on (001)Pt/(001)MgO substrate. (a) Reciprocal space map of (004)PZT. Clear diffraction peak is confirmed, indicating the PZT film is grown with the epitaxial relationship to the (001)Pt/(001)MgO substrate. (b) Reciprocal space map of (204)PZT. The solid line represents the relationship of lattice parameters  $a=c$ . The peak position of (204)PZT is located below this line, indicating  $c$  axis is longer than  $a$  axis.

strate removal. To evaluate the stress-free PZT films, Rietveld analysis was performed to identify the detailed structure.<sup>11</sup> In the case of the bulk PZT, the structural parameter was reported in detail by the structural refinement of neutron-diffraction patterns<sup>12</sup> and recently, Noheda *et al.* discovered a monoclinic phase near the morphotropic phase boundary (MPB) using Rietveld analysis for the synchrotron XRD measurements.<sup>13</sup> In this study, we adopted this method to characterize the intrinsic structure of the PZT thin film with a rhombohedral composition of Zr/Ti=68/32, free from the clamping of the substrate as the base material to predict their electric properties.

## II. EXPERIMENT

The PZT films were deposited using rf-sputtering technique at a substrate temperature of  $\sim 830$  K. The deposition rate was as high as  $1 \mu\text{m/h}$  and we prepared relatively thick films of  $3.9 \mu\text{m}$  to suppress the clamping effects of the substrate. The target composition was Zr/Ti of 70/30 with 20% excess PbO to compensate for Pb reevaporation from the films. We measured the film composition using a wavelength dispersive x-ray spectroscopy (WDS: JEOL JXA-8900R). In the measurement, the film composition was determined as  $\text{Pb}_{1.15}(\text{Zr}_{0.68}\text{Ti}_{0.32})_{0.85}\text{O}_3$ , indicating excess Pb still existed in the as-grown films. Since the Curie temperature of bulk PZT

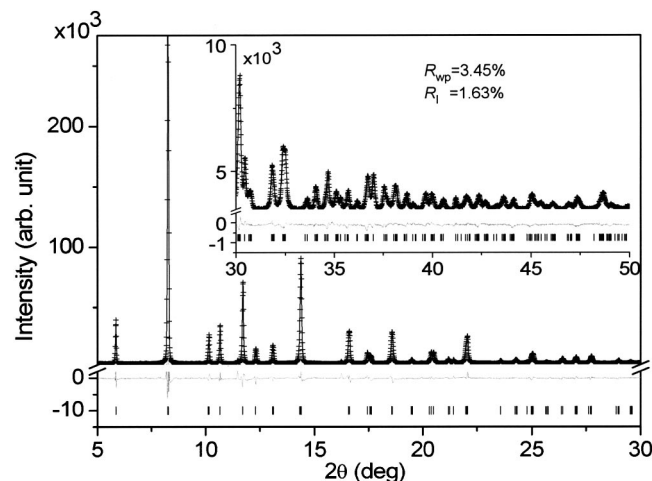


FIG. 2. Synchrotron XRD patterns of the powdered PZT (Zr/Ti=68/32) films at room temperature. Observed (+), calculated patterns by Rietveld refinement (solid line), and the difference curve (gray line) were plotted. When the calculation is conducted as the space group of PZT is  $R3m$ , a satisfactory fit could be obtained ( $R_{wp}=3.45\%$ ,  $R_i=1.63\%$ ).

with Zr/Ti of 68/32 is about 610 K,<sup>14</sup> the films were grown with the cubic structure and phase transition to ferroelectric phase should occur in a cooling process.

To identify the crystalline structure of the PZT films on Pt/MgO substrates,  $2\theta/\theta$  XRD measurements were performed using Cu  $K\alpha 1$  ( $1.5405 \text{ \AA}$ ) radiation. Furthermore, four-circle XRD measurements were also conducted to determine the in-plane lattice parameters and the crystalline phase.

After removing the substrate, we examined the intrinsic crystalline structure of the PZT films. The MgO substrate was etched away using  $\text{H}_3\text{PO}_4$  solution and residual PZT/Pt film was ground into powder. The crystalline structure of the powdered PZT/Pt film was measured using the x-ray of synchrotron radiation to obtain adequate diffraction intensity from a small amount of the samples. The powder was packed into a quartz capillary tube with an internal diameter of  $0.2 \text{ mm}$ . The diffraction measurements were carried out using BL02B2 beam line at the Japan Synchrotron Radiation Research Institute (SPring-8).<sup>15</sup> The x-ray of wavelength  $0.4205 \text{ \AA}$  from a precollimator mirror and a double-crystal monochromator were used with the large-diameter Debye-Scherrer camera of radius  $278 \text{ mm}$ . The resulting angular resolution was  $0.02^\circ$ . The diffraction patterns were analyzed by the Rietveld method using a program of RIETAN.<sup>16</sup>

## III. RESULTS

### A. Structural characterization of stress-free PZT films

In the  $2\theta/\theta$  XRD measurements, we observed strong (00 $l$ ) diffraction peaks and no other orientations and phases like pyrochlore even though excess Pb existed in the films. Furthermore, four-circle XRD measurements revealed that the PZT films were grown with the epitaxial relationship to the substrates. The reciprocal space maps of (004) and (204)PZT reflections were shown in Figs. 1(a) and 1(b). The diffraction peak of (204)PZT is located under the line of  $Q_z=2Q_x$  passing through the peaks of (204)MgO and

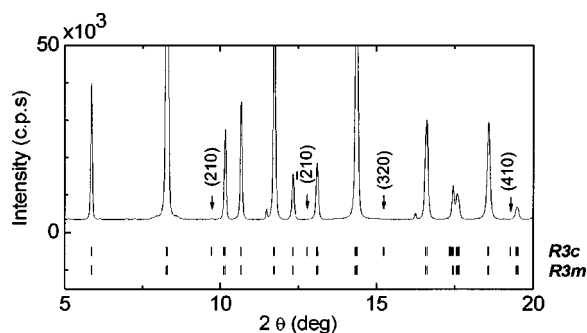


FIG. 3. Comparison of the peak position of  $R3c$  and  $R3m$ . The reflections of (210),  $(\bar{2}10)$ , (302), and (410) in  $R3c$  could not be observed in the experimental pattern.

(204)Pt, indicating PZT films with Zr/Ti of 68/32 show the tetragonal structure on the substrates even though the Zr/Ti composition is in the stable rhombohedral region in bulk PZT.<sup>14</sup> The lattice constant of the  $a$  axis was calculated as 4.08 Å, while that of the  $c$  axis was 4.15 Å. In the previous study, we have found that the epitaxial PZT films with almost the same composition showed the tetragonal structure on (001)Pt/(001)SrTiO<sub>3</sub> substrates, while (111)-oriented epitaxial PZT films on (111)Pt/(111)SrTiO<sub>3</sub> substrates showed the rhombohedral structure due to the isotropic stress to each lattice.<sup>17</sup> These results indicate that the stress from the substrates still deforms the crystalline structure even though the film thickness is around 3.9 μm.

Figure 2 shows the XRD patterns of powdered PZT films at room temperature using synchrotron radiation. The crystalline structure was refined using the Rietveld method under the condition of anisotropic temperature factors for Pb and isotropics for Zr/Ti and O. The occupation factor  $g$  of Pb and Zr/Ti in both the A and B site of the ABO<sub>3</sub> structure was also optimized as  $g_{\text{Zr/Ti}}^{\text{A}} = 1 - g_{\text{Pb}}^{\text{A}}$  and  $g_{\text{Pb}}^{\text{B}} = 1 - g_{\text{Zr/Ti}}^{\text{B}} = 1.15 - g_{\text{Pb}}^{\text{B}}$ , where superscripts indicate the atomic position of the perovskite unit and subscripts are the elements. Since the film composition of Pb/(Zr+Ti) ratio was 1.15/0.85, the occupation factors of each element can be described as  $g_{\text{Pb}}^{\text{A}} + g_{\text{Pb}}^{\text{B}} = 1.15$  and  $g_{\text{Zr/Ti}}^{\text{A}} + g_{\text{Zr/Ti}}^{\text{B}} = 0.85$ . The sample contains powdered Pt electrode and we analyzed the diffraction patterns as PZT and Pt system. The lattice parameter of Pt is calculated to be 3.9225 Å, which is the same value of bulk Pt. This result implies that the powdered sample is fully relaxed from the internal stress by substrate clamping.

The structure refinements demonstrated that the powdered PZT film was returned to the rhombohedral phase with a satisfactory fit of agreement factor  $R_{\text{wp}} = 3.45\%$ . This result indicates that the restriction of the substrate actually distorts the crystalline structure even in the film thickness as thick as

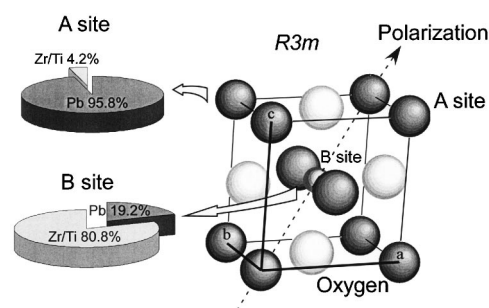


FIG. 4. Refined structure of powdered  $\text{Pb}_{1.15}(\text{Zr}_{0.68}\text{Ti}_{0.32})_{0.85}\text{O}_3$  films. 19.2% of the B site was occupied by Pb atoms, while 4.2% of the A site is occupied by Zr/Ti atoms. The lattice parameter of  $a = 4.12167$  Å is slightly larger than that of bulk PZT [4.113 Å:  $\text{Pb}(\text{Zr}_{0.70}\text{Ti}_{0.30})\text{O}_3$ ] due to the intrusion of large Pb atoms in the B site.

3.9 μm, although it was reported that the stress from the substrate was relaxed above the thickness of 0.5 μm for the epitaxial ferroelectric films.<sup>18</sup> The space group of the powdered PZT film can be determined as  $R3m$  since some of the specific diffraction peaks of  $R3c$ , which is the normal structure of bulk PZT(68/42) at room temperature, cannot be observed and the diffraction pattern is in good agreement with  $R3m$ , as shown in Fig. 3. Furthermore, the profile analysis indicates that the Pb atoms, which usually occupy the A site, intrude on 19% of the B site, while a small amount of Zr/Ti atoms also occupied 4% of the B site, as depicted in Fig. 4. For comparison, calculations were conducted on the assumption that the excess Pb was locally segregated or dispersively existed like interstitial atoms, but agreement factors of  $R_{\text{wp}}$  and  $R_i$  became larger compared with the case of cation-exchanged PZT. The volume of the perovskite unit cell was derived as 70.02 Å<sup>3</sup>, which is larger than the bulk PZT(70/30) of 69.58 Å<sup>3</sup>,<sup>12</sup> supporting the analytical results of intrusion of large Pb atoms into the B site, which caused the cell volume swelling. Table I summarizes the structural parameters of powdered PZT films obtained by Rietveld refinements.

## B. Phase transition

In order to investigate phase transition, we observed the diffraction patterns of the powdered PZT films ranging from 92 to 700 K. Figure 5(a) shows the temperature dependence of the volume of the perovskite unit cell. The increasing rate of the volume is clearly changed at 600 K, indicating that above this temperature the phase transformation from rhombohedral to cubic phase occurs. The rhombohedral tilt angle  $\alpha$  gradually increases with increasing temperature, as shown in Fig. 5(b). Although above 500 K tilt angle was not con-

TABLE I. Structure refinement results for epitaxial  $\text{Pb}_{1.15}(\text{Zr}_{0.68}\text{Ti}_{0.32})_{0.85}\text{O}_3$  films free from the substrates with space-group  $R3m$ .

Atom	Site	$g$	$x$	$y$	$z$
Pb/M	A	0.958(6)/0.042	0	0	0
Pb/M	B	0.192(6)/0.808	0.5348(8)	0.5348(8)	0.5348(8)
O		1.0	0.574(4)	0.574(4)	0.036(8)
$a = 4.12167(7)$ Å, $\alpha = 89.8240(9)^\circ$ , $M = \text{Zr}_{0.68} + \text{Ti}_{0.32}$					



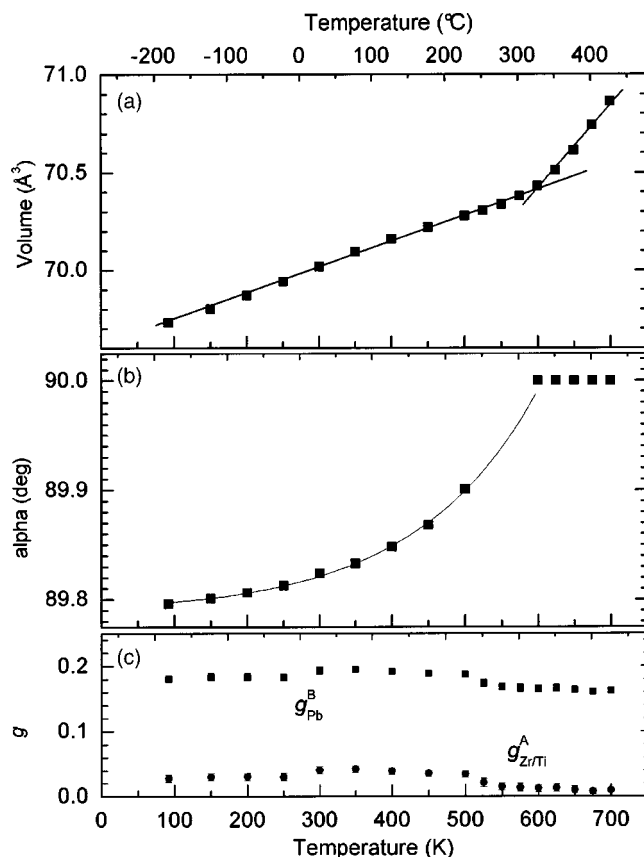


FIG. 5. Temperature dependence of the crystalline structure of powdered  $\text{Pb}_{1.15}(\text{Zr}_{0.68}\text{Ti}_{0.32})_{0.85}\text{O}_3$  ranging from 92 to 700 K. (a) The volume of the perovskite unit cell as a function of temperature. The increasing rate is clearly changed at 600 K, where phase transition from  $R3m$  to  $Pm3m$  occurs. (b) The rhombohedral tilt angle  $\alpha$  as a function of temperature. The  $\alpha$  gradually increases with the temperature and the extrapolation curve reaches  $90^\circ$  at 600 K, which is consistent with the dependence of the cell volume. (c) The occupation factors of  $g_{\text{Zr/Ti}}^{\text{A}}$  and  $g_{\text{Pb}}^{\text{B}}$  as a function of temperature. The occupation ratios of Zr/Ti and Pb in the A and B sites are almost constant to the temperature; however, slight decreases are observed at higher temperature probably due to the thermal annealing effects.

verged well in the calculation, the extrapolation curve is reached to  $90^\circ$  at the temperature of 600 K, which is consistent with the result of the volume dependence. The transition temperature of powdered PZT films is slightly lower than that of bulk PZT ( $\sim 610$  K) probably due to the anomalous crystalline structure of stress-free PZT films whose cations are exchanged in the A and B sites. On the other hand, occupation factors  $g_{\text{Zr/Ti}}^{\text{A}}$  and  $g_{\text{Pb}}^{\text{B}}$  are almost constant, but slightly decrease at higher temperature due to thermal annealing effects, as shown in Fig. 5(c).

#### IV. DISCUSSION

The profile refinement of the stress-free PZT films demonstrated that the intrinsic crystalline structure of the PZT films returned from the tetragonal to the rhombohedral phase by substrate removal, but its space group was identified not as  $R3c$  but as  $R3m$ . In addition, mixing of the Pb and Zr/Ti cations in the A and B sites was also found out. These results suggest that the stress from the substrate is not the only factor for the distortion of the crystalline structure of the thin films.

The anomalous structure of the stress-free PZT films is attributed to the deposition process of the thin films. The growth of the thin films suffers in-plane stress during the deposition, while bulk materials are usually crystallized under isotropic pressure field. When the PZT thin film is deposited on the flat surface of the substrate, the films inevitably suffer in-plane stress even at the initial stage of the deposition and, furthermore, the  $c$  axis tends to be perpendicular to the  $a$ - $b$  plane due to the in-plane stress during the cooling process. This fact implies that the epitaxial growth of the PZT thin films progresses with the distorted structure, and the intrusion of Pb atoms in the B site probably minimizes the growth energy. Another possible reason is the exposure of rf plasma and the bombardment of energetic sputtered species, which enhance nonthermal equilibrium reactions during film growth. Deposition by sputtering or pulsed laser deposition (PLD) uses energetic species ejected from the target; therefore, the bombardment to the surface of the films induces abrupt heating and cooling conditions, which lead to anomalous crystallization. In fact, significant distorted structure has been observed for the epitaxial ferroelectric films deposited by sputtering and PLD.<sup>17,18</sup> Whatever the cause may be, the crystalline structure of the stress-free epitaxial films is different from the bulk one, and the effect of the internal stress should be considered as the extrinsic factor on the basis of the intrinsic stress-free structure of the films.

#### V. CONCLUSION

In this study, we have revealed the intrinsic structure of the epitaxial PZT thin films with Zr/Ti composition of 68/42. Reitveld analysis of the synchrotron XRD measurements is a very useful technique to determine the detailed crystalline structure of the thin-film materials released from the substrates. The deformation of the crystalline structure is actually caused by the in-plane stress due to the clamping effect of the substrate as an extrinsic factor. However, the stress-free PZT films show a different crystalline structure from the bulk materials, especially as the site exchange of cation atoms was identified. The anomalous crystalline structure of the stress-free PZT films induces the slight decrease of the phase-transition temperature. These results suggest that the stress effect for the PZT thin films should be considered on the basis of the intrinsic stress-free structure of the films.

#### ACKNOWLEDGMENTS

This work was supported by the Industrial Technology Research Grant Program in 2004 from NEDO and COE program of the Ministry of Education, Culture, Sports, Science and Technology, Japan. The synchrotron radiation experiments were performed on BL02B2 at Spring-8 with the approval of the JASRI (Grant No. 2002B0710-ND1-np).

- <sup>1</sup>J. -P. Locquet, J. Perret, J. Fompeyrine, E. Machler, J. Seo, and G. Van Tendeloo, *Nature (London)* **394**, 453 (1998).
- <sup>2</sup>M. Abrecht, D. Ariosa, D. Cloetta, S. Mitrovic, M. Onellion, X. X. Xi, G. Margaritondo, and D. Pavuna, *Phys. Rev. Lett.* **91**, 057002 (2003).
- <sup>3</sup>C. M. Foster, G.-R. Bai, R. Csencsits, J. Vetrone, R. Jammy, L. A. Wills,

- E. Carr, and J. Amano, J. Appl. Phys. **81**, 2349 (1997).
- <sup>4</sup>B. S. Kwak, A. Erbil, B. J. Wilkens, J. D. Budai, M. F. Chisholm, and L. A. Boatner, Phys. Rev. Lett. **68**, 3733 (1992).
- <sup>5</sup>B. S. Kwak, A. Erbil, J. D. Budai, M. F. Chisholm, L. A. Boatner, and B. J. Wilkens, Phys. Rev. B **49**, 14865 (1994).
- <sup>6</sup>J. Wang *et al.*, Science **299**, 1719 (2003).
- <sup>7</sup>M. J. Haun, E. Furman, S. J. Jang, H. A. McKinsry, and L. E. Cross, J. Appl. Phys. **62**, 3331 (1987).
- <sup>8</sup>M. J. Haun, E. Furman, S. J. Jang, and L. E. Cross, Ferroelectrics **99**, 13 (1989).
- <sup>9</sup>S. H. Oh and H. M. Jang, Phys. Rev. B **63**, 132101 (2001).
- <sup>10</sup>T. Matsunaga, T. Hosokawa, Y. Umetani, R. Takayama, and I. Kanno, Phys. Rev. B **66**, 064102 (2002).
- <sup>11</sup>H. M. Rietveld, J. Appl. Crystallogr. **2**, 65 (1969).
- <sup>12</sup>D. L. Corker, A. M. Glazer, R. W. Whatmore, A. Stallard, and F. Fauth, J. Phys.: Condens. Matter **10**, 6257 (1998).
- <sup>13</sup>B. Noheda, J. A. Gonzalo, L. E. Cross, R. Guo, S.-E. Park, D. E. Cox, and G. Shirane, Phys. Rev. B **61**, 8687 (2000).
- <sup>14</sup>B. Jaffe, W. R. Cook, and H. Jaffe, *Piezoelectric Ceramics* (Academic, London, 1971), p. 136.
- <sup>15</sup>E. Nishiboria *et al.*, Nucl. Instrum. Methods Phys. Res. A **467-468**, 1045 (2001).
- <sup>16</sup>F. Izumi, J. Crystallogr. Soc. Jpn. **27**, 23 (1985).
- <sup>17</sup>I. Kanno, H. Kotera, K. Wasa, T. Matsunaga, T. Kamada, and R. Takayama, J. Appl. Phys. **93**, 4091 (2003).
- <sup>18</sup>T. Zhao, F. Chen, H. Lu, G. Yang, and Z. Chen, J. Appl. Phys. **87**, 7442 (2000).